Supersonic Flutter Analysis of Functionally Graded Material Plates with Cracks

S Natarajan[*1], G Manickam[2], S Bordas[3]

[1]School of Civil and Environmental Engineering, University of New South Wales, Sydney, NSW, Australia

[2]Stress & DTA, Bombardier Aerospace India Center, IES-Aerospace, Mahindra Satyam Computers Services Ltd., Bangalore, India

[3]Institute of Mechanics and Advanced Materials, Cardiff University, Wales, UK

[*1]sundararajan.natarajan@gmail.com; [2]mganapathi@rediffmail.com; [3]stephane.bordas@gmail.com

Abstract

In this paper, the flutter behaviour of functionally graded material plates immersed in a supersonic flow is studied. An enriched 4-noded quadrilateral element based on field consistency approach is used for this study. The crack is modelled independent of the underlying mesh using partition of unity method (PUM), the extended finite element method (XFEM). The material properties are assumed to be graded only in the thickness direction and the effective material properties are estimated using the rule of mixtures. The plate kinematics is described based on the first order shear deformation theory (FSDT) and the shear correction factors are evaluated employing the energy equivalence principle. The influence of the crack length, the crack orientation, the flow angle and the gradient index on the aerodynamic pressure and the frequency are numerically studied. The results obtained here reveal that the critical frequency and pressure decrease with increase in crack the length and are minimum when the crack is aligned to the flow angle.

Keywords

Supersonic Flutter; Extended Finite Element Method; Numerical Integration; Crack; Flow Angle; Functionally Graded Material

Introduction

The emergence of functionally graded materials (FGMs) that combine the best properties of its constituent materials (for example, ceramics and metals) is considered to be an alternative to certain class of aerospace structures exposed to high temperature environment. FGMs are characterized with a smooth transition from one material to another, thus circumventing high inter-laminar shear stresses and delamination problem that persists in laminated composites. With the increased use of these materials, it necessitates to study the dynamic characteristics of the structures made up of FGMS.

Background

It can be seen from the literature that the introduction of FGMs has attracted researchers to investigate the structural behaviour of such structures. Analytical solutions are proposed based on the three-dimensional solutions and second-order shear deformation theory. Different plate theories, viz., FSDT, second and other higher order accurate theory have been used to describe the plate kinematics. The static and dynamic fracture mechanics study of FGMs have been studied in the literature. Dolbow and Gosz employed the XFEM to compute mixed mode stress intensity factors. However, such analysis of plates is scarce in the literature. Huang et al., have analysed the vibration of side-cracked FGM thick plate analytically by employing Ritz procedure, whereas, Natarajan et al., examined the FGM plate with through center crack using the XFEM. Chau-Dinh et al., and Rabczuk et al., employed phantom node methods and meshfree methods with external enrichment to study the response of shells with arbitrary cracks.

Since FGMs are seen as potential candidates for aircraft structural applications, it is important to understand the dynamic characteristics of structures made up of such materials when exposed to air flow. Prakash and Ganapathi studied the linear flutter characteristics of FGM panels exposed to supersonic flow. Haddadpour et al., and Sohn and Kim investigated the nonlinear aspects of flutter characteristics using the finite element method. It can be seen from the available literature that the work on flutter characteristics of FGM plates with cracks, to the author's knowledge is not available. Earlier studies on flutter characteristics of cracked isotropic and composite panels employed finite element procedure. Although these numerical studies give insight into the

understanding of flutter behaviour, the method requires the mesh to conform to the geometry. This inherently limits the analyses to fixed calculation parameters.

Approach

In this paper, we apply the XFEM to model the crack independent of the underlying mesh and then to study the flutter behaviour of FGM plates immersed in a supersonic flow based on the FSDT. Here, an enriched four noded Co shear flexible quadrilateral plate element based on the consistency approach is used to analyse the flutter behaviour. To the author's knowledge the flutter characteristics of FGM plates with arbitrary cracks has not been studied earlier. The influence of the crack length, the crack orientation, the flow direction and the material property on the evaluation of critical speed and the type of fluttering instability is numerically studied.

Outline

The paper is organized as follows, the next section will give an introduction to FGM and a brief overview of Reissner-Mindlin plate theory. The spatial discretization and the basic idea of the XFEM are presented in Section 3. Section 4 presents results for the flutter analyses of cracked functionally graded material panels, followed by concluding remarks in the last section.

Formulation

Functionally Graded Material

A rectangular plate made up of a mixture of ceramic and metal is considered with the coordinates x,y along the in-plane directions and z along the thickness direction (see Figure 1). The material on the top surface ($z = h/2$) of the plate is ceramic and graded to metal at the bottom surface ($z=-h/2$) by a power law distribution. The effective Young's modulus E and Poisson's ratio γ of the FGM, evaluated using the rule of mixtures as: $E = E_c V_c + E_m V_m$ and $\gamma = \gamma_c V_c + \gamma_m V_m$, where $V_i(i=c,m)$ is the volume fraction of the phase material. The subscripts c and m refere to ceramic and metal phases respectively. The volume fraction of the ceramic and metal phases are related by $V_c + V_m = 1$ and V_c is expressed as, $V_c(z) = [(2z+h)/2h]^k$, where k is the volume fraction exponent ($k > 0$), also called the gradient index.
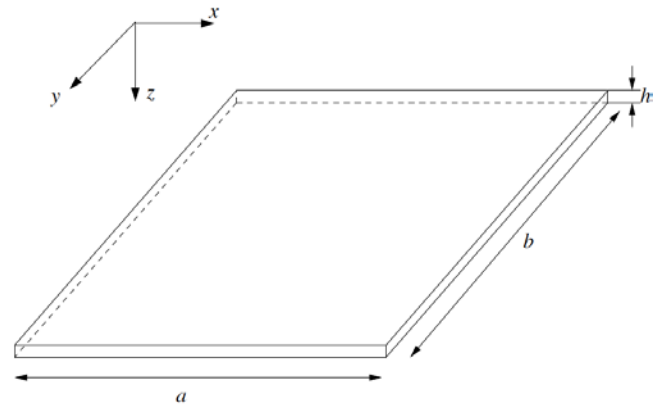
Reissner-Mindlin Plate Theory

Using Mindlin formulation, the displacements (u,v,w) at a point (x,y,z) in the plate from the medium surface are expressed as functions of midplane displacements (u_o,v_o,w_o) and independent rotations β_x and β_y of the normal in xz and yz planes, respectively as:

$$u(x, y, z, t) = u_o(x, y, t) + z\beta_x(x, y, t)$$
$$v(x, y, z, t) = v_o(x, y, t) + z\beta_y(x, y, t)$$
$$w(x, y, z, t) = w_o(x, y, t)$$

(1)

The midplane membrane strains ε_p, the bending strains ε_b and the shear strain ε_s are written as

$$\varepsilon_p = \left\{ \begin{array}{c} u_{o,x} \\ v_{o,y} \\ u_{o,y} + v_{o,x} \end{array} \right\}, \varepsilon_b = \left\{ \begin{array}{c} \beta_{x,x} \\ \beta_{y,y} \\ \beta_{x,y} + \beta_{y,x} \end{array} \right\}.$$

$$\varepsilon_s = \left\{ \begin{array}{c} \beta_x + w_{o,x} \\ \beta_y + w_{o,y} \end{array} \right\}.$$

(2)

where the subscript `comma' represents the partial derivative with respect to the spatial coordinate succeeding it. The strain energy of the plate can be expressed in terms of the field variables $\delta = (u_o,v_o,w_o,\beta_x,\beta_y)$ and their derivatives as:

$$U(\delta) = \frac{1}{2} \int_\Omega \left\{ \varepsilon_p^T \mathbf{A} \varepsilon_p + \varepsilon_p^T \mathbf{B} \varepsilon_b + \varepsilon_b^T \mathbf{B} \varepsilon_p + \varepsilon_b^T \mathbf{D}_b \varepsilon_b + \varepsilon_s^T \mathbf{E} \varepsilon_s \right\} \, d\Omega$$

(3)

where the matrices $\mathbf{A},\mathbf{B},\mathbf{D}_b$ and $\mathbf{E}$ are the extensional, bending-extensional coupling, bending and transverse shear stiffness coefficients. The kinetic energy of the plate is given by:

$$T(\boldsymbol{\delta}) = \frac{1}{2} \int_\Omega \left\{ I_o(\dot{u}_o^2 + \dot{v}_o^2 + \dot{w}_o^2) + I_1(\dot{\theta}_x^2 + \dot{\theta}_y^2) \right\} \, d\Omega$$

(4)

where $I_o = \int_{-h/2}^{h/2} \rho(z) \, dz$, $I_1 = \int_{-h/2}^{h/2} z^2 \rho(z) \, dz$ and $\rho(z)$ is the mass density that varies through the thickness of the plate. The work done by the applied non-conservative load is:

$$W(\boldsymbol{\delta}) = \int_\Omega \Delta pw \, d\Omega$$

(5)

where Δp is the aerodynamic pressure. The aerodynamic pressure based on first order, high Mach number approximation to linear potential flow is given by:

$$\Delta p = \frac{\rho_a U_a^2}{\sqrt{M_\infty^2 - 1}} \left[w_{,x} \cos \theta' + w_{,y} \sin \theta' + \chi \dot{w} \right]$$

(6)

where $\chi = \left(\frac{1}{U_a} \right) \frac{M_\infty^2 - 2}{M_\infty^2 - 1}$, ρ_a, U_a, M_∞ and θ' are the free stream air density, velocity of the air, Mach number and the flow angle, respectively. The static aerodynamic approximation for Mach numbers between $\sqrt{2}$ and 2 is obtained by setting $\dot{w} = \partial w / \partial t$ to zero in Equaiton (6). The governing equations obtained using the minimization of total potential energy are solved based on the finite element method. The finite element equations thus derived are:

$$\left[(\mathbf{K} + \lambda \overline{\mathbf{A}}) - \omega^2 \mathbf{M} \right] \boldsymbol{\delta} = \mathbf{0}$$

(7)

where $\mathbf{K}$ is the stiffness matrix, $\mathbf{M}$ is the consistent mass matrix, $\lambda = \frac{\rho_a U_a^2}{\sqrt{M_\infty^2 - 1}}$, $\overline{\mathbf{A}}$ is the aerodynamic force matrix and ω is the natural frequency. When $\lambda = 0$, the eigenvalue of ω is real and positive, since the stiffness matrix and the mass matrix are symmetric and positive definite. However, the aerodynamic matrix $\overline{\mathbf{A}}$ is unsymmetric and hence complex eigenvalues ω are expected for $\lambda > 0$. As λ increases monotonically from zero, two of these eigenvalues will approach each other and become complex conjucates. In this study, λ_{cr} is considered to be the value of λ at which the first coalescence occurs.

Spatial Discretization

The plate element employed here is a C^o continuous shear flexible field consistent element with 5 degrees of freedom $(u_o, v_o, w_o, \beta_x, \beta_y)$ at four nodes in a 4-noded bilinear quadrilateral (QUAD-4) element. The shear locking behaviour is suppressed by using the field redistributed substitute shape functions to interpolate the shear strains. The conventional polynomial expansion of the displacement field fails to capture the local behaviour of the problem. The basic idea in the XFEM is to append the conventional expansion of the displacement field with additional functions. The additional functions, also called the `enrichment functions' carry additional information regarding the local behaviour. In general, the field variables are approximated by:

$$\mathbf{u}^h(\mathbf{x}) = \sum_{I \in \mathcal{N}^{\text{fem}}} N_I(\mathbf{x}) \mathbf{q}_I + \text{enrichment functions}$$

(8)

where $N_I(\mathbf{x})$ are the standard finite element shape functions and $\mathbf{q}_I$ are the nodal variables associated with node I. The following enriched approximation proposed by Dolbow et al., for the plate displacements are used:

$$(u^h, v^h, w^h)(\mathbf{x}) = \sum_{I \in \mathcal{N}^{\text{fem}}} N_I(\mathbf{x})(u_I^s, v_I^s, w_I^s) +$$
$$\sum_{J \in \mathcal{N}^c} N_J(\mathbf{x}) H(\mathbf{x})(b_J^u, b_J^v, b_J^w) +$$
$$\sum_{K \in \mathcal{N}^f} N_K(\mathbf{x}) \left(\sum_{l=1}^4 (c_{Kl}^u, c_{Kl}^v, c_{Kl}^w) G_l(r, \theta) \right)$$

(9)

The section rotations are approximated by:

$$\beta_x^h(\mathbf{x}) = \sum_{I \in \mathcal{N}^{\text{fem}}} \tilde{N}_{1I}(\mathbf{x}) \beta_{xI}^s + \sum_{J \in \mathcal{N}^c} \tilde{N}_{1J}(\mathbf{x}) H(\mathbf{x}) b_J^{\beta_x}$$
$$+ \sum_{K \in \mathcal{N}^f} \tilde{N}_{1K}(\mathbf{x}) \left(\sum_{l=1}^4 c_{Kl}^{\beta_x} F_l(r, \theta) \right)$$
$$\beta_y^h(\mathbf{x}) = \sum_{I \in \mathcal{N}^{\text{fem}}} \tilde{N}_{2I}(\mathbf{x}) \beta_{yI}^s + \sum_{J \in \mathcal{N}^c} \tilde{N}_{2J}(\mathbf{x}) H(\mathbf{x}) b_J^{\beta_y}$$
$$+ \sum_{K \in \mathcal{N}^f} \tilde{N}_{2K}(\mathbf{x}) \left(\sum_{l=1}^4 c_{Kl}^{\beta_y} F_l(r, \theta) \right)$$

(10)

where $\mathcal{N}^{\text{fem}}$ is a set of all nodes in the finite element mesh, $\mathcal{N}^c$ is a set of nodes that are enriched with the Heaviside function, $H(\mathbf{x})$ and $\mathcal{N}^f$ are a set of nodes that are enriched with near tip asymptotic fields, $G_l(r, \theta)$ and $F_l(r, \theta)$. In Equations (9) and (10), $(u_I^s, v_I^s, w_I^s, \beta_{xI}^s, \beta_{yI}^s)$ are the nodal unknown vectors associated with the continuous part of the finite

element solution, b_J is the nodal enriched degree of freedom vector associated with the Heaviside (discontinuous) function and c_{Kl} is the nodal enriched degree of freedom vector associated with the elastic asymptotic near-tip functions.

A special care must be taken to numerically integrate the stiffness matrix due to the addition of non-polynomial functions. The standard Gauss quadrature cannot be applied to elements enriched by discontinuous terms, because Gauss quadrature implicitly assumes a polynomial approximation. In the present study, a triangular quadrature with sub-division aligned to the discontinuity surface is employed. For the elements that are not enriched, a standard 2x2 Gaussian quadrature rule is used. The other techniques that can be employed are Schwarz Christoffel Mapping, Generalized quadrature and the Smoothed eXtended FEM.

Results and Discussion

In this section, we present the critical aerodynamic pressure and the critical frequency of a cracked simply supported FGM panels using the extended Q4 formulation. The element has five nodal degrees of freedom $(u_o, v_o, w_o, \beta_x, \beta_y)$. A full integration scheme is applied to evaluate the various strain energy terms. A simply supported boundary condition is assumed for the current study given by: $u_o = w_o = \beta_y = 0$ on $x = 0, a$; $v_o = w_o = \beta_x = 0$ on $y = 0, b$. In all cases, we present the non dimensionalized critical aerodynamic pressure λ_{cr} and critical frequency ω_{cr} as $\omega_{cr} = \Omega_{cr} a^2 \sqrt{\frac{\rho_c h}{D_c}}, \lambda_{cr} = \bar{\lambda}_{cr} \frac{a^3}{D_c}$, unless specified otherwise, where $D_c = \frac{E_c h^3}{12(1-\nu_c^2)}$ is the bending rigidity of the plate. The subscript c refers to the material property corresponding to the ceramic phase. For this study, the plate thickness is assumed to be a/h=100. The effect of material property, the crack orientation θ, the crack length d/a and the flow angle θ' on the flutter behaviour are studied numerically. Based on a progressive mesh refinement, a 34x34 structured quadrilateral mesh is found to be adequate to model the full plate for the present analysis. The FGM plate considered here consists of silicon nitride (Si₃N₄) and stainless steel (SUS304). The Young's modulus and the mass density for Si₃N₄ are $E_c = 348$ GPa, $\rho_c = 2370$ Kg/m³ and for SUS304 are $E_m = 201.04$ GPa and $\rho_m = 8166$ Kg/m³. Poisson's ratio γ is assumed to be constant and taken as 0.3.

TABLE 1 COMPARISON OF CRITICAL AERODYNAMIC PRESSURE AND COALESCENCE FREQUENCY FOR AN ISOTROPIC PLATE WITH VARIOUS BOUNDARY CONDITIONS (SSSS – ALL EDGES SIMPLY SUPPORTED, CCCC – ALL EDGES CLAMPED) AND (A/B = 1, A/H = 100, Υ = 0.3, Θ' = 0°)

	Flutter Bounds	Boundary condition	
		SSSS	CCCC
Prakash and Ganapathi (2006)	λ_{cr}	511.11	852.34
	ω_{cr}	1840.29	4274.32
Present	λ_{cr}	513.48	854.80
	ω_{cr}	1849.50	4297.00

Before proceeding with the detailed study, the formulation developed herein is validated against available results pertaining to the critical aerodynamic pressure and the critical frequency for an isotropic plate without a crack. The computed critical aerodynamic pressure and the critical frequency for an isotropic square plate with various boundary conditions are given in Table 1. It can be seen that the results from the present formulation are in good agreement with those in the literature
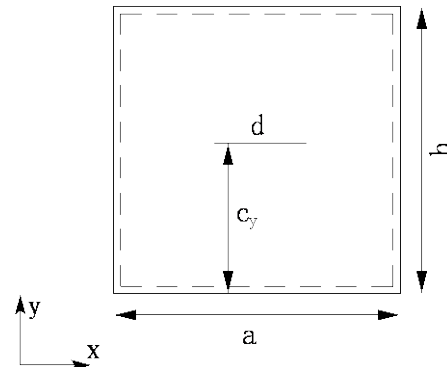

FIG. 2 SIMPLY SUPPORTED PLATE WITH A CENTER CRACK

Next, the flutter characteristics of square simply supported cracked FGM plates is investigated. Consider a plate of uniform thickness, h and with length and width as a and b, respectively. Figure 2 shows a plate with all edges simply supported with a center crack of length d and a distance of c_y from the x-axis. In this example, the influence of the crack length d/a, the crack orientation θ, the flow angle θ' and the gradient index k on the critical aerodynamic pressure and the critical frequency is studied. Figure 3 shows the variation of the critical aerodynamic pressure λ_{cr} and the critical frequency ω_{cr} with gradient index for a center horizontal crack of length $d/a = 0.5$ in a normal flow $\theta' = 0^o$. It can be seen that with increasing gradient index, both the critical aerodynamic pressure and the critical frequency decreases. This is because of the stiffness degradation due to increase in the

metallic volume fraction. Figure 4 shows the influence of the crack length d/a on the critical aerodynamic pressure and the critical frequency. It is observed that as the crack length increases, the critical aerodynamic pressure and the critical frequency decreases. This is due to the fact that increasing the crack length increases the local flexibility and thus decreases the frequency. It can be seen that the combined effect of increasing the crack length and the gradient index is to lower the critical frequency and the critical pressure. It can also be observed from Figure 3 that the critical pressure and the frequency drop sharply for slight increase in the metallic volume fraction, but with further increase in the metallic volume fraction, the drop in the pressure and the frequency is marginal. In both cases, the decrease in the critical aerodynamic pressure and the critical frequency is due to the stiffness degradation.
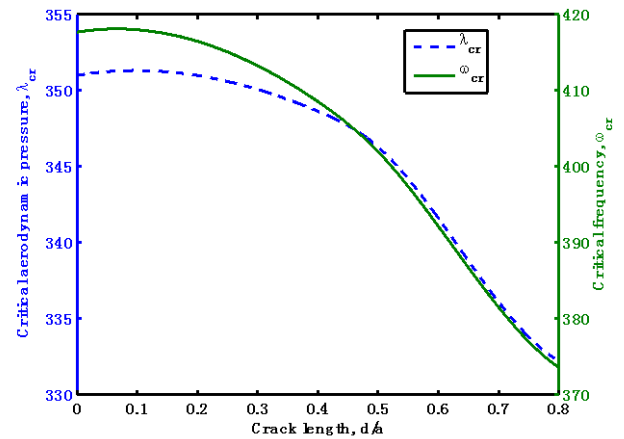

FIG. 4 THE CRITICAL AERODYNAMIC PRESSURE λ_{cr} AND THE CRITICAL FREQUENCY ω_{cr} AS A FUNCTION OF CRACK LENGTH d/a FOR A SIMPLY SUPPORTED SQUARE FGM PLATE WITH A CENTER HORIZONTAL CRACK IN A NORMAL FLOW $\theta' = 0^o$ WITH GRADIENT INDEX $k=5$.
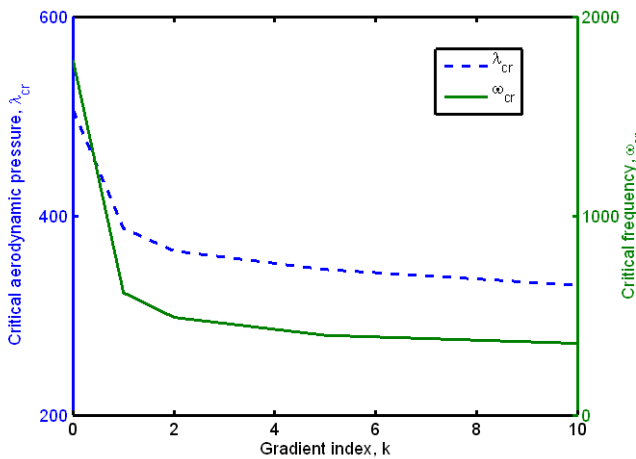

FIG. 3 VARIATION OF CRITICAL AERODYNAMIC PRESSURE λ_{cr} AND THE CRITICAL FREQUENCY ω_{cr} WITH GRADIENT INDEX IN A NORMAL FLOW $\theta'=0^o$ FOR A SIMPLY SUPPORTED SQUARE FGM PLATE WITH A CENTER HORIZONTAL CRACK WITH d/a = 0.5.

Figure 5 shows the influence of the crack angle θ on the critical pressure and the frequency for a simply supported square FGM plate with gradient index $k = 0$, immersed in a normal flow $\theta'= 0^o$. From Figure 5, it can be seen that with increase in the crack orientation, the critical pressure increases gradually until the crack is oriented at right angles to the flow angle and with further increase in the crack orientation, the critical pressure and the frequency decreases. Further, it is observed that the critical pressure is the lowest for a crack orientation $\theta=0^o$ and 180°. At these crack orientations, the crack is aligned to the flow direction. The critical frequency and the pressure values tend to be symmetric with respect to a crack orientation $\theta = 90^o$.
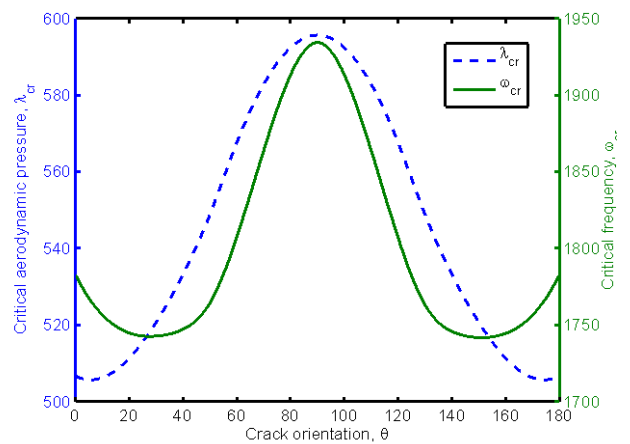

FIG. 5 CRITICAL AERODYNAMIC PRESSURE λ_{cr} AS A FUNCTION OF CRACK ORIENTATION FOR A SIMPLY SUPPORTED SQUARE FGM PLATE WITH A CENTER CRACK $d/a = 0.5$ IN A NORMAL FLOW $\theta'= 0^o$ AND GRADIENT INDEX $k=0$.
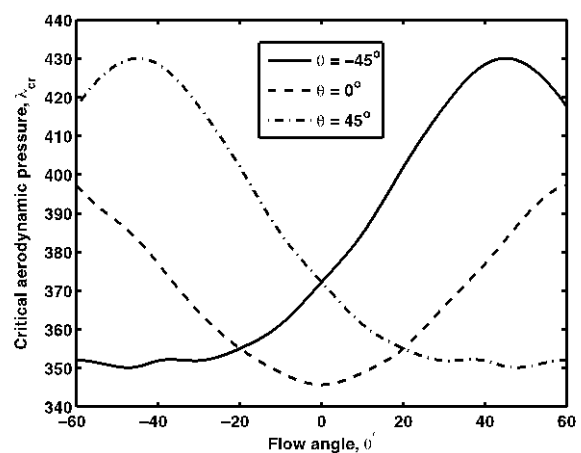

FIG. 6 EFFECT OF FLOW ANGLE θ' ON THE CRITICAL AERODYNAMIC PRESSURE FOR A SIMPLY SUPPORTED SQUARE FGM PLATE WITH A CENTER HORIZONTAL CRACK WITH $d/a = 0.5$ AND GRADIENT INDEX $k = 5$.

The influence of the flow angle on the critical pressure for a simply supported square FGM plate with gradient index $k = 5$ is shown in Figure 6 for different crack orientations, i.e, $\theta = -45^o, 0^o$ and $+45^o$. It is observed that the critical pressure is minimum when the crack is aligned to the flow angle. The critical frequency increases for other flow angles irrespective of the orientation of the crack.

Conclusions

The flutter characeristics of cracked FGM panels immersed in a supersonic flow has been analysed based on the first order shear deformation theory within the framework of the extended finite element approach. The aerodynamic force is accounted for assuming the first-order Mach number approximation potential flow theory and the homogenized material properties are estimated by rule of mixtures. Numerical experiments have been conducted to bring out the effect of the gradient index, the crack length, the crack orientation and the flow angle on the flutter characteristics of the FGM panel. From the detailed numerical study, it can be concluded that with increasing gradient index and the crack length, the critical pressure and the critical frequency decreases. In both cases, the decrease is due to the stiffness degradation. It is also observed that the critical frequency and the pressure are minimum when the crack is aligned to the flow.

REFERENCES

Babusˇka, I. and Melenk. J. "The partition of unity finite element method." International Journal for Numerical Methods in Engineering 40 (1997): 727–758.

Belytschko, T. and Black, T. "Elastic crack growth in finite elements with minimal remeshing." International Journal for Numerical Methods in Engineering 45 (1999): 601–620.

Birman, V. and Librescu, L. "Supersonic flutter of shear deformation laminated flat panel." Journal of Sound and Vi- bration 139 (1990): 265–275.

Bordas, S., Natarajan et al., S. "On the performance of strain smoothing for quadratic and enriched finite element approximations (XFEM/GFEM/PUFEM)." Internaitonal Journal for Numerical Methods in Engineering 86 (2011): 637-666.

Chau-Dinh, T., Zi, G., Lee, P., Song, J. and Rabczuk, T. "Phantom-node method for shell models with arbitrary cracks." Computers & Structures 92–93 (2012): 242–256.

Chen, W. and Lin, H. "Flutter analysis of thin cracked panels using the finite element method." AIAA Journal 23 (1985): 795–801.

Dixon, S. "Comparison of panel flutter results from approximate aerodynamic theory with results from exact theory and experiment." Tech. Rep. TN D-3649, NASA (1966).

Dolbow, J. and Gosz, M. "On the computation of mixed-mode stress intensity factors in functionally graded materials." International Journal of Solids and Structures 39 (2002): 2557–2574.

Dolbow, J., Moe¨ s, N. and Belytschko, T. "Modeling fracture in mindlin-reissner plates with the extended finite element method." International Journal of Solids and Structures 37 (48-50) (2000): 7161–7183.

Ferreira, AJM., Batra, RC., Roque, CMC., Qian, LK. and Jorge, RMN. "Natural frequencies of function- ally graded plates by a meshless method." Composite Structures 75 (2006): 593–600.

Ganapathi, M., Varadan, T. and Sarma, B. "Nonlinear flexural vibrations of laminated orthotropic plates." Computers and Structures 39 (1991): 685–688.

Haddadpour, H., Navazi, H. and Shadmehri, F. "Nonlinear os- cillations of a fluttering functionally graded plate." Composite Structures 79 (2007): 242–250.

Huang, C., III, OM. and Chang, M. "Vibrations of cracked rectangular FGM thick plates." Composite Structures 93 (2011): 1747–1764.

Matsunaga, H. "Free vibration and stability of function- ally graded plates according to a 2-D higher-order deformation theory." Composite Structures 82 (2008): 499–512.

Mousavi, SE. and Sukumar, N. "Numerical integration of polynomials and discontinuous functions on irregular convex polygons and polyhedrons." Computational Mechanics 47 (2011): 535-554.

Natarajan, S. and Manickam, G. "Bending and vibration of functionally graded material sandwich plates using an accurate theory." Finite Elements in Analysis and Design 57 (2012): 32–42.

Natarajan, S., Baiz, P., Bordas, S., Rabczuk, T. and Kerfriden, P. "Natural frequencies of cracked functionally graded material plates by the extended finite element method." Composite Structures 93 (2011): 3082–3092.

Natarajan, S., Baiz, P., Ganapathi, M. and Bordas, S. "Linear free flexural vibration of cracked functionally graded plates in thermal environment." Computers and Structures 89 (2011): 1535–1546.

Natarajan, S., Bordas, S. and Mahapatra, DR. "Numerical integration over arbitrary polygonal domains based on Schwarz Christoffel conformal mapping." International Journal for Numerical Methods in Engineering 80 (2009): 103-134.

Nazari, M.B., Shariati, M., Eslami, M.R. and Hassani, B. "Computation of stress intensity factor in functionally graded plates under thermal shock." Journal of Mechanical Engineering 57 (2011): 622–632.

Pidaparti, R. and Chang, C. "Finite element supersonic flutter analysis of skewed and cracked composite panels." Computers and Structures 69 (1998): 265–270.

Prakash, T. and Ganapathi, M. "Supersonic flutter characteristics of functionally graded flat panels including thermal effects." Composite Structures 72 (2006): 10–18.

Qian, L.C., Batra, R.C. and Chen, L.M. "Static and dynamic deformations of thick functionally graded elastic plates by using higher order shear and normal deformable plate theory and Meshless Local Petrov Galerkin Method, Composites Part B: Engineering 35 (2004): 685-697.

Rabczuk, T. and Areias, P. "A meshfree thin shell for arbitrary evolving cracks based on an external enrichment." Computer Modeling in Engineering and Sciences 16 (2) (2006): 115–130.

Rabczuk, T., Areias, P. and Belytschko, T. "A meshfree thin shell method for nonlinear dynamic fracture." International Journal for Numerical Methods in Engineering 72 (2007): 524–548.

Reddy, J.N. "Analysis of functionally graded plates." International Journal for Numerical Methods in Engineering 47 (2000): 663-684.

Shiau, L "Flutter of composite laminated beam plates with delamination." AIAA Journal 30 (1992): 2504– 2511.

Sohn, K.-J. and Kim, J. "Structural stability of functionally graded panels subjected to aero-thermal loads." Composite Structures 82 (2008): 317–325.

Sohn, K.-J. and Kim, J. "Nonlinear thermal flutter of functionally graded panels under a supersonic flow." Com- posite Structures 88 (2009): 380–387.

Somashekar, B., Prathap, G., and Babu, CR. "A field-consistent four-noded laminated anisotropic plate/shell element." Computers and Structures 25 (1987): 345–353.

Strganac, T. and Kim, Y. "Aeroelastic behavior of composite plates subjected to damage growth." Journal of Aircraft 33 (1996): 68–73.

Sundararajan, N., Prakash, T. and Ganapathi, M. "Nonlinear free flexural vibrations of functionally graded rectangular and skew plates under thermal environments." Finite Elements in Analysis and Design 42 (2) (2005): 152– 168.

Vel, S.S. and Batra, RC. "Three-dimensional exact solu- tion for the vibration of functionally graded rectangular plates." Journal of Sound and Vibration 272 (2004): 703–730.

Vel, S.S. and Batra, RC. "Exact solutions for thermoelas- tic deformations of functionally graded thick rectangu- lar plates." AIAA J 40 (2002): 1421–1433.

Yang, J. and Shen, H.S. "Vibration characteristic and transient response of shear deformable functionally graded plates in thermal environments." Journal of Sound and Vibration 255 (2002) 579-602.